Earth Science
2013; 2(5): 104-112
Published online September 20, 2013 (http://www.sciencepublishinggroup.com/j/earth)
doi: 10.11648/j.earth.20130205.11

Investigating the structures within the Lower Benue and Upper Anambra basins, Nigeria, using first Vertical Derivative, Analytical Signal and (CET) centre for exploration targeting plug-in

ADETONA, A. ABBASS[1, *], ABU MALLAM[2]

[1]Department of Physics, Federal University of Technology Minna
[2]Department of Physics, University of Abuja, Abuja

Email address:
tonabass@yahoo.com(A. A. ABBASS), mallamabu@yahoo.com(A. MALLAM)\

To cite this article:
ADETONA, A. ABBASS, ABU MALLAM. Investigating the Structures within the Lower Benue and Upper Anambra Basins, Nigeria, Using First Vertical Derivative, Analytical Signal and (CET) Centre for Exploration Targeting Plug-In. *Earth Science*. Vol. 2, No. 5, 2013, pp. 104-112. doi: 10.11648/j.earth.20130205.11

Abstract: The IGRF-corrected 2009 aeromagnetic data over the Lower Benue and Upper Anambra basins Nigeria was subjected to both Vertical and Horizontal Derivatives, Analytical Signal and CET grid analysis, these digital processing tools were achieved both on map and profile analysis. From the analysis of both the Vertical and Horizontal Derivatives the study area could be divided into two regions based on the degree of distortion to the magnetic signatures the Northern and the Western edge of the area is covered by short wavelength magnetic anomalous signatures that are the characteristic of outcrop and shallow intrusive magnetic bodies, while the remaining part of the study area is characterized by medium to long wavelength magnetic signatures that are attributes of deep sited magnetic rocks in areas of medium to thick sedimentations. Result of the Analytical Signal which is in local amplitude reveals regions with outcrop of magnetic rocks having amplitudes ranging from 0.230 to 0.40 (shown as pink color), area with magnetic rock intruding into sedimentary formations at shallow depths, with amplitudes ranging from 0.094 to 0.229 cycles (shown as red color), while regions with magnetic rock intruding into sedimentary formations at greater depths, having very low amplitudes ranging from -0.085 to 0.055 cycles (shown in yellow to green color). Analyses due to CET grid analysis equally reveal the basement rocks to the North and Southern edge of the study area. Intrusions into the sedimentary formation are also revealed. The research discovered that the lower (southern) part of the area (on Angba and Otukpo area) shows structures (Basaltic rocks) that intrude into the basement which could have predate the sedimentation period, several fracture and fault lines are detected on the CET map, most prominent among them is that at the Southeastern corner of the area which trends NE-SW which can be attributed to an onshore extension of Charcots fault zone , and that which trends N-S is a fault line that controls the course of River Niger. These three features are responsible for the depressions where sediments can accumulate.

Keywords: International Geomagnetic Reference Field (IGRF), Basaltic Intrusions, Source Parameter Imaging, Horizontal Gradient and Center for Exploration Targeting (CET)

1. Introduction

Knowledge of the geology of a region is the scientific basis for resource exploration (petroleum, solid minerals, groundwater) the world over. Among the variety of rock types to be found in the Earth's crust, many exhibit magnetic properties, whether a magnetization induced by the present-day geomagnetic field, or a remnant magnetization acquired at some time in the geological past, or a combination of both. Mapping the patterns of magnetic anomalies attributable to rock magnetism has proved to be a very effective way of reconnaissance large areas of geology at low cost per unit area. The fact that most sedimentary rocks and surface-cover formations (including water) are effectively nonmagnetic means that the observed anomalies are attributable to the underlying igneous and metamorphic rocks (the so-called "magnetic basement"), even where they are concealed from direct observation at the surface. Anomalies arising from the magnetic basement are only diminished in amplitude and extended in wavelength through the extra vertical distance between source and magnetometer imposed by the nonmagnetic sediment layers. Thus aeromagnetic surveys are able to indicate the distribution of bedrock lithologies and structures virtually everywhere. Interpretation of magnetic anomaly patterns can then lead to maps of (hidden) geology that give direction to the exploration process. [1,2] While aeromagnetic surveys are extensively used as reconnaissance tools, there has been an increasing recognition of their value for evaluating prospective areas by virtue of the unique information they provide. [3], outline the roles of aeromagnetic survey as follows:

i. Delineation of volcano-sedimentary belts under sand or other recent cover, or in strongly metamorphosed terrains when recent lithologies are otherwise unrecognizable.
ii. Recognition and interpretation of faulting, shearing and fracturing not only as potential hosts for a variety of minerals, but also an indirect guide to epigenetic, stress related mineralization in the surrounding rocks.
iii. Identification and delineation of post-tectonic intrusive. Typical of such targets are zoned syenite or carbonatite complexes, kinerlites, tin-bearing granites and mafic intrusions.
iv. Direct detection of deposits of certain iron ores.
v. In prospecting for oil, aeromagnetic data can give information from which one can determine depths to basement rocks and thus locate and define the extent of
vi. sedimentary basins. Sedimentary rocks however exert such a small magnetic effect compared with igneous rocks that virtually all variations in magnetic intensity measurable at the surface result from topographic or lithologic changes associated with the basement or from igneous intrusions [1].

2.1. Location and Extent of the Study Area

The study area covers the Lower Benue Trough, the Upper part of Anambra Basin and the basement complexes bounding it at the West and Northern edges. The area is bounded by Latitude 7.0^0N to 8.5^0N and Longitude 6.5^0E to 8.5^0E. The physiological features recognized in the area are the river Benue, river Anambra and river Okulu. Twelve aeromagnetic maps covered the study area and are numbered, (227, 228, 229, 230, 247, 248, 249, 250, 267, 268, 269 and 270), A total area of 36,300 square kilometers. The study area touches four states majorly, which are Nassarawa at the upper part, Kogi, Enugu and Benue States at the lower part, Fig 1.

2.2. Geology of Lower Benue and Upper Anambra Basin

Sedimentation in the Lower Benue Trough commenced with the marine Albian *Asu River Group*, although some pyroclastics of Aptian – Early Albian ages have been sparingly reported [4]. The Asu River Group in the Lower Benue Trough comprises the shales, limestones and sandstone lenses of the Abakaliki Formation in the Abakaliki area and the Mfamosing Limestone in the Calabar Flank [5]. The marine Cenomanian – Turonian *Nkalagu Formation* (black shales, limestones and siltsones) and the interfingering regressive sandstones of the *Agala* and Agbani Formations rest on the Asu River Group. Mid-Santonian deformation in the Benue Trough displaced the major depositional axis westward which led to the formation of the Anambra Basin.

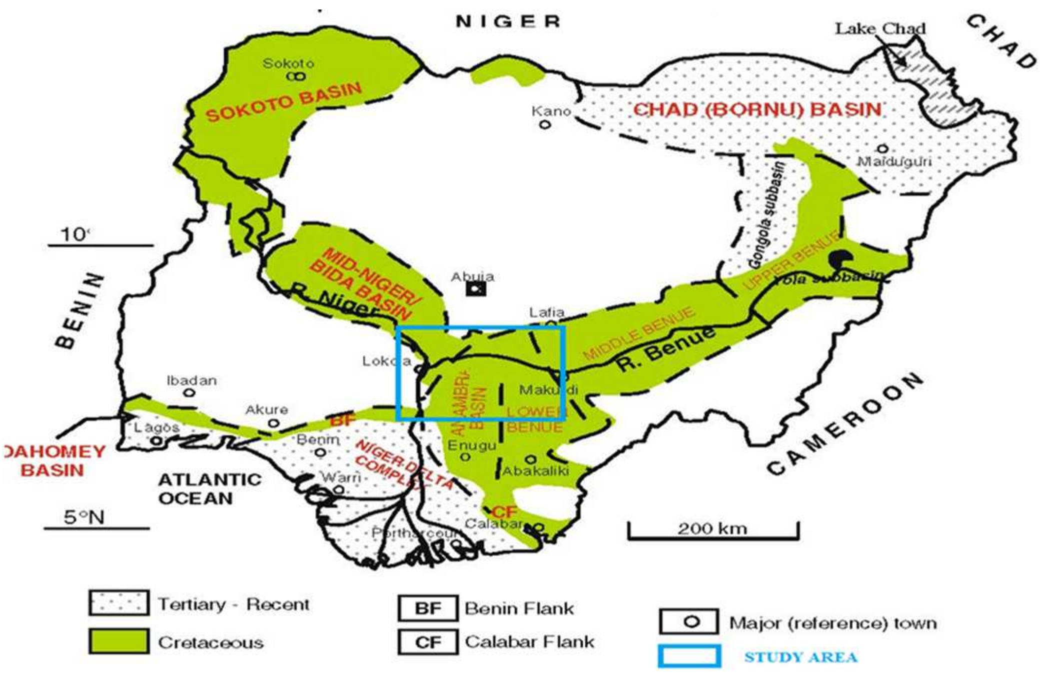

***Fig1:** Cretaceous to Recent sediments representing the third phase of marine sedimentation in the Benue Trough (Ladipo, 1988; Akande and Erdtmann,).*

Post-deformational sedimentation in the Lower Benue Trough, therefore, constitutes the Anambra Basin. Sedimentation in the Anambra Basin thus commenced with the Campanian-

Maastrichtian marine and paralic shales of the Enugu and Nkporo Formations,overlain by the coal measures of the Mamu Formation. The fluviodeltaic sandstones of the Ajali and Owelli Formations lie on the Mamu Formation and constitute its lateral equivalents in most places. In the Paleocene, the marine shales of the Imo and Nsukka Formations were deposited, overlain by the tidal Nanka Sandstone of Eocene age. Downdip, towards the Niger Delta, the Akata Shale and the Agbada Formation constitute the Paleogene equivalents of the

Anambra Basin (Figs.3)

The Basin Formation and the Imo Shale mark the onset of another transgression in the Anambra during the aleocene. The shales contain significant amount of organic matter and may be potential source for the hydrocarbons in the northern part of the Niger Delta. In the Anambra Basin, they are only locally expected to reach maturity levels for hydrocarbon expulsion.

The Enugu and the Nkporo Shales represent the brackish marsh and fossiliferous pro-delta facies of the Late Campanian-Early Maastrichtian depositional cycle [5]**.** Deposition of the sediments of the Nkporo/Enugu Formations reflects a funnel-shaped shallow marine setting that graded into channeled low-energy marshes. The coal-bearing Mamu Formation and the Ajali Sandstone accumulated during this epoch of overall regression of the Nkporo cycle. The Mamu Formation occurs as a narrow strip trending north–south from the Calabar Flank, swinging west around the Ankpa plateau and terminating at Idah near the River Niger The best exposure of the Nkporo Shale is at the village of Leru

(Lopauku). The Ajali Sandstone marks the height of the regression at a time when the coastline was still concave. The converging littoral drift cells governed the

*sed*imentation and are reflected in the tidal sand waves which are characteristic for the 72 km south of Enugu on the Enugu – Portharcourt express road, while that of Enugu Shale is at Enugu, near the Onitsha-Road flyover . Fig: 2

The Mamu Formation is best exposed at the

Miliken Hills in Enugu, with well-preserved secions along the road cuts from the King Petrol Station up the Miliken Hills and at the left bank of River Ekulu.

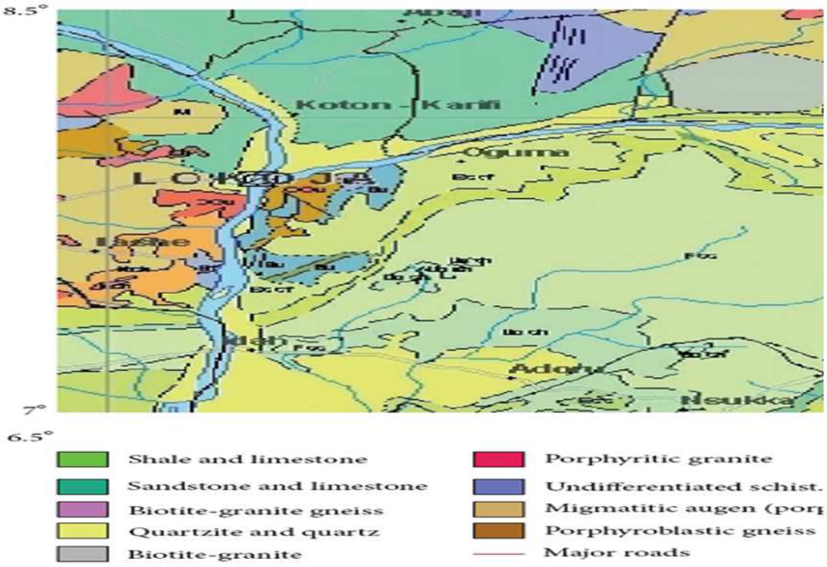

Fig 2: *Geology map of the study area (adopted from geological and mineral map of ,2009 Nigeria Geological Survey agency.*

3. Main Body

3.1. Source of Aeromagnetic Data

A new dataset has been generated from the largest airborne geophysical survey ever undertaking in Nigeria, which is helping to position the country as an exciting destination for explorers. This survey which was conducted in three phases between 2005 and 2009 was partly financed the Nigerian Federal Government and the World Bank as part of a major project known as the Sustainable Management for Mineral Resources Project. All of the airborne geophysical work: data acquisition processing and compilation was carried out by Fugro Airborne Surveys the survey acquire both magnetic and radiometric data compilation. The recent survey has a Tie-line spacing of 500 meters, flight line spacing of 100 meters and Terrain clearance of 80 meters using TEMPEST system. Compared with the 1970's survey which has a Tie-line spacing of 20 km, flight line spacing of 2 km and flying altitude of 200 m, these levels of survey are intensive and detail for the objectives of this research. Data covering the twelve aeromagnetic sheets numbered (227, 228, 229, 230, 247, 248, 249, 250, 267, 268, 269 and 270) was acquired from "The Nigerian Geological Survey Agency. 31, Shetima Mangono Crescent Utako District P.M.B 616, Garki Abuja.

3.2. Method

The procedures employed in this research include:

1. Production of Total Magnetic Intensity (TMI) map of the study area in color aggregate using Oasis montaj software.
2. Computing the First Vertical Derivative of TMI reduced to pole and manually locating identified structures on the map.
3. Computing the Horizontal Derivatives in the X,Y and Z directions
4. Compute the Euler's equation using the Horizontal Derivatives (DX,DY and DZ) to compute the Analytical Signal
5. Application of Centre for Exploration Targeting (CET) Grid Analysis Plug-In for Structural analysis

3.3. Theory of Method

3.3.1. Euler Deconvolution

Euler deconvolution is an automatic technique used for locating the source of potential field based on both their amplitudes and gradients. The method was developed by [6] to interpret 2D magnetic anomalies and extended by [7] to be used on grid-based data. Magnetic field *M* and its spatial derivatives satisfy Euler's equation of homogeneity.

$$(x-x_0)\frac{\partial M}{\partial x}+(y-y_0)\frac{\partial M}{\partial y}+(z-z_0)\frac{\partial M}{\partial z}=-NM, \qquad (1)$$

where $\frac{\partial M}{\partial x}, \frac{\partial M}{\partial y}$ and $\frac{\partial M}{\partial z}$ represent first-order derivative of the magnetic field along the x-, y- and z- directions, respectively, *N* is known as a structural index and related to the geometry of the magnetic source. For example, *N*=3 for sphere, *N*=2 for pipe, *N*=1 for thin dike and *N*=0 for magnetic contact [6]. Taking into account a base level for the regional magnetic field (B), equation (1) can be rearranged and written as

$$x_0\frac{\partial M}{\partial x}+y_0\frac{\partial M}{\partial y}+z_0\frac{\partial M}{\partial z}+NB=x\frac{\partial M}{\partial x}+y\frac{\partial M}{\partial y}+z\frac{\partial M}{\partial z}+NM., \qquad (2)$$

Assigning the structural index *(N)*, a system of linear equations can be obtained and solved for estimating the location and depth of the magnetic body. Using a moving window, multiple solutions from the same source can be obtained. Good solutions are considered to be those that cluster well and have small standard deviations [6,7]. Selection of the appropriate structural index is very important to obtain the correct depth solutions. However, the estimated horizontal location is independent of the structural index [8], which means that there is no ambiguity with regard to the structural location.

3.3.2. Analytical Signal

This filter when applied to the Total Magnetic Intensity data is aimed at simplifying the fact that magnetic bodies usually have positive and negative peak associated with it, which may make it difficult to determine the exact location of causative body. For two dimensional bodies a bell shaped symmetrical function is derived and for a three dimensional bodies the function is amplified of analytical signal. This function and it derivatives are independent of strike dip magnetic declination, inclination and remanent magnetization [9].

The 3.D analytical signal A of a potential field anomaly can be defined [10].

$$A(x,y,z)=\left[\frac{\partial M}{\partial x}\right]x+\left[\frac{\partial M}{\partial y}\right]y+\left[\frac{\partial M}{\partial z}\right]z \qquad (3)$$

Where *M* = magnetic field.

3.3.2. The Centre for Exploration Targeting (CET) Grid Analysis Plug-In For Structures

The aim of structural analysis is to:

1. Locate the contact between the basement at the north and western part and the sedimentary region of the study area
2. Locate the extent and position of the outcrops and intrusive bodies (into basement and sedimentary formations) within the study area
3. Detect fracture or any fault that may exist within the area
4. Interpret entire the lineaments detected.

Starting with the Standard deviation that provides an estimate of the local variations in the data. At each location in the grid, it calculates the standard deviation of the data values within the local neighborhood. Features of significance often exhibit high variability with respect to the background signal. For a window containing *N* cells, whose mean value is μ, the standard deviation σ of the cell values x_i is given by:

$$\sigma=\sqrt{\frac{1}{N}\sum_{i=1}^{N}(x_i-\mu)^2} \qquad (4)$$

When interpreting the output, values which approach zero indicate very little variation, whereas large values indicate high variation. The next stage is to apply Phase Symmetry; this property is useful in detecting line-like features through identifying axes of symmetry. It is also known that the symmetry of a signal is closely related to the periodicity of its spatial frequency. Consequently, it is natural to utilize a frequency-based approach to detect axes of symmetry. This plug-in implements the phase symmetry algorithm developed by [11].

In the one-dimensional case (1D), a point of symmetry in the spatial domain corresponds with a point where local frequency components are at either a minimum or a maximum. To identify points of symmetry in two-dimensional (2D) data we first break the data into 1D profile and analyze these over multiple orientations at varying scales. For example, a line-like feature will produce strong symmetry responses from the 1D profiles sampled from all orientations except for those parallel to the line. The result from phase symmetry is passed through Amplitude Thresholding, in conjunction with non-maximal suppression (NMS). The NMS is useful for finding ridges since low values are suppressed whilst points of local maxima are preserved, it also takes into account the local feature orientation so that the continuity of features is maximized and can be used to remove noise and highlight linear features. A description of the NMS algorithm is given below.

For each cell in the grid, it examines the values at a distance, *r*, in the directions perpendicular to the local feature orientation - the local feature orientation is typically the direction in which a ridge or valley is running. If the cell has a value greater than those on either side of it, the cell is kept since it is a local maximum; otherwise it is set to zero.

The Amplitude Thresholding plug-in applies the above algorithm followed by a thresholding step. Thresholding marks cells in grid as either 'foreground' or 'background' cells depending on whether the cell value is greater or less than a specified threshold value respectively. Thus thresholding will reduce a grid to a binary grid of only two distinct cells values: 1 for regions of interest and a dummy value for background.

In this suite of tools, Amplitude Thresholding is useful for reducing phase symmetry or phase congruency output to a grid depicting only trend lines.

Finally Skeleton to Vectors is applied. The Skeleton to Vectors plug-in is for vectorising the skeletonised structures from the skeletonisation plug-in via a line fitting method described below. This vectorised data can then be used as input to the structural complexity map plug-ins. For each structure in the grid, a line is formed between its start and end points. If the structure deviates from this line by more than a specified tolerance the structure is divided into two at the point of maximum deviation and the line fitting process is repeated on these two new structure segments. This process is continued recursively until no structure segment deviates from its corresponding line segment by more than the specified tolerance. These line segments form the vectorised representation of the structures within the grid [12].

4. Results and Discussions

4.1. Interpretation of Structures Identified from First Vertical Derivative and Analytical Signal Maps

The magnetic intensity the area ranges from -2415.97 minimum to 1264.72 maximum with an average value of 33.87 nT for a total of 3,667251 data points.Fig:3 The area is marked by both high and low magnetic closures, which could be attributed to several factors such as (1) variation in depth (2) difference in magnetic susceptibility (3) difference in lithology (4) degree of strike.

Structural trends within the study area are N-E and NE-SW (First vertical Derivative of the TMI). Fig: 4 High Frequency (short wavelength) signatures observed at the Northern and Western portion of the study area revealed a shallow depth to magnetic source typical of Basement Complex. Long wavelength signatures observed at the major part of the study area is as a result of deep magnetic source typical of Sedimentary basin.

The striking feature with NW-SE trending maximum negative magnetic anomaly zone in the northern part of basin is associated with Sonakhan greenstone belt Undifferentiated Older granite, mainly porphyritic buried under the sediments. granite granitized gneiss with porphyroblastic granite. Rock type at the Northern portion is identified as Biotite gneiss. False bedded sandstone, coal, sandstone and shale. (Ajali Formation). Coal, sandstone and shale formation identified around Otukpa, Abejukolo and Ofugo in Kogi State; Abaji in FCT; Udegi and Amaku in Nasarawa State and areas in Benue and Enugu States.

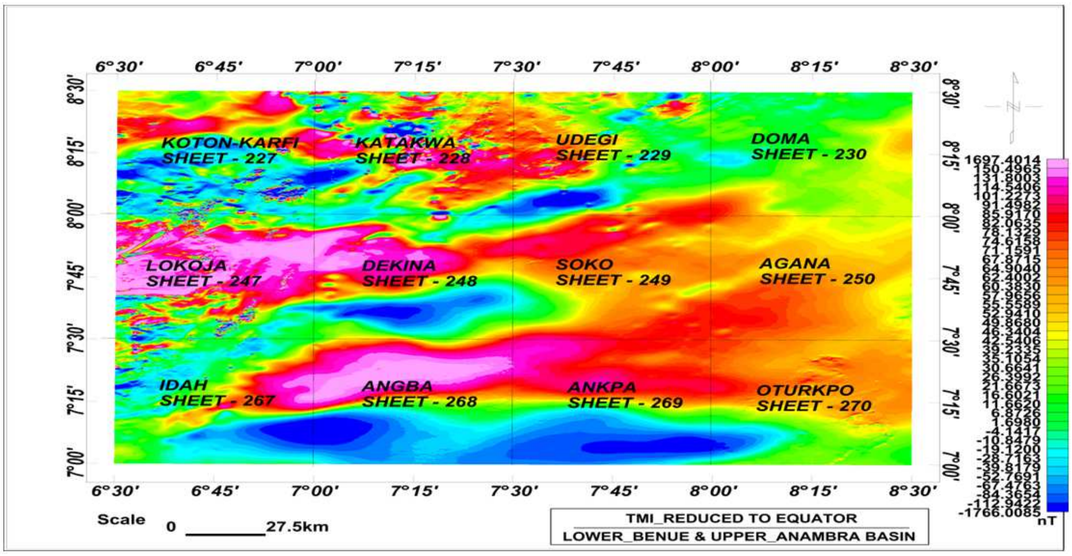

Fig 3: *Total Magnetic Intensity (TMI) Map of the Study Area*

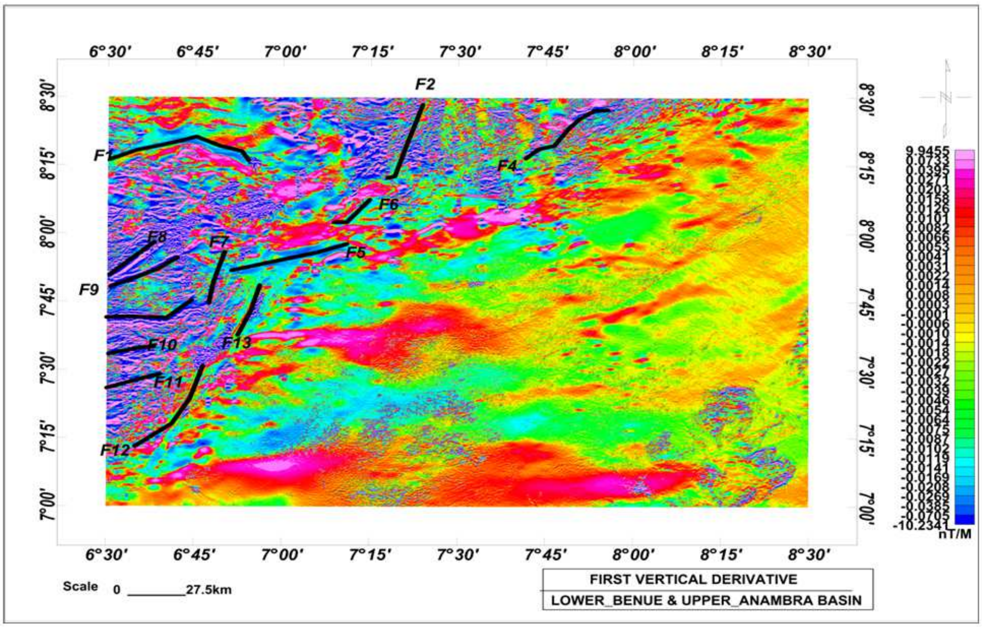

Fig 4: *First Vertical Derivative Map Showing Identified Structures*

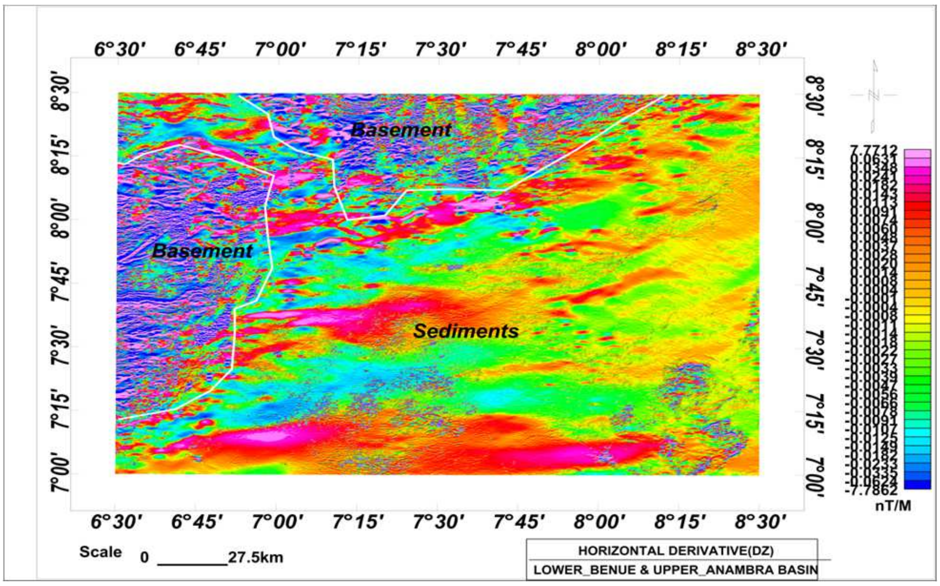

Fig 5: *Horizontal Derivative Map (DZ) Showing Contacts*

Rock type at the western portion of the study area is identified from geology image Fig: 2 as Undifferentiated Older granite, mainly porphyritic granite granitized gneiss with porphyroblastic granite. Rock type at the Northern portion is identified as Biotite gneiss. False bedded sandstone, coal, sandstone and shale are the lithologic units at the surface within the sedimentary basin.

River Alluvium deposition identified along the river channel. [13]

4.2. Application of Analytical Signal for Structural Analysis and Result

In this research we applied the method using the structural index (SI=1) of contact or step [7, 14], window size of 10 and flight height 100 meters, since the main objective is to map structures Figure 6**.** The result is amplitude domain with regions having outcrops with high amplitude values ranging from 0.257 to 0.4 cycles (shown as pink color). Regions with magnetic rock intruding into sedimentary formations at shallow depths, having medium amplitudes ranging from 0.094 to 0.229 cycles (shown as red color). While regions with magnetic rock intruding into sedimentary formations at greater depths, having very low amplitudes ranging from -0.085 to 0.055 cycles (shown in yellow to green color).

4.3. Application of CET Grid Analysis Plug-In and Results

Application of the standard deviation and the phase symmetry plug-in produces the map in Fig. 7 while applications of the amplitude thresholding and the skeleton to vectors plug-in yield the map in fig: 8. The following basic features can be deduced from figures 7 and figure 8:-

Outcrop of undifferentiated older granite, mainly porphyritic granite granitized gneiss with porphyroblastic granite, at the Western part of the map. While the Northern part consist of intrusions of rocks identified as Biotite gneiss. False bedded sandstone, coal, sandstone and shale are the lithologic units at the surface within the lower sedimentary basin. Contact between these basement rocks and the sedimentary formation is visibly defined.

At the lower mid-portion and Eastern corner of the map located structures that are Basaltic rocks that intrude into the basement it is believe than these structures must have predate the depositional period of the sedimentary formation

Two major fault lines can be identified on figures 7 and 8 a vertically running fault line that structurally define the course of river Niger within the area, and the extension of Chain's fault line that cuts the South East corner of the study area. Combination of the three features above could have course the depression responsible for the basin formation.

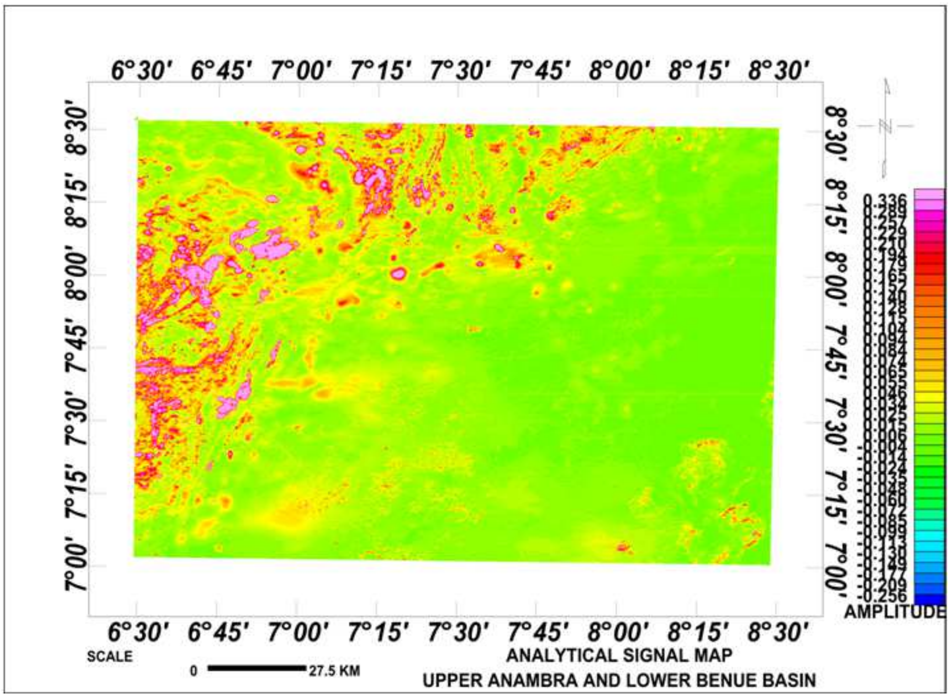

Fig. 6: *3_D-Analytical Signal Map from Euler's solutions of the Study Area*

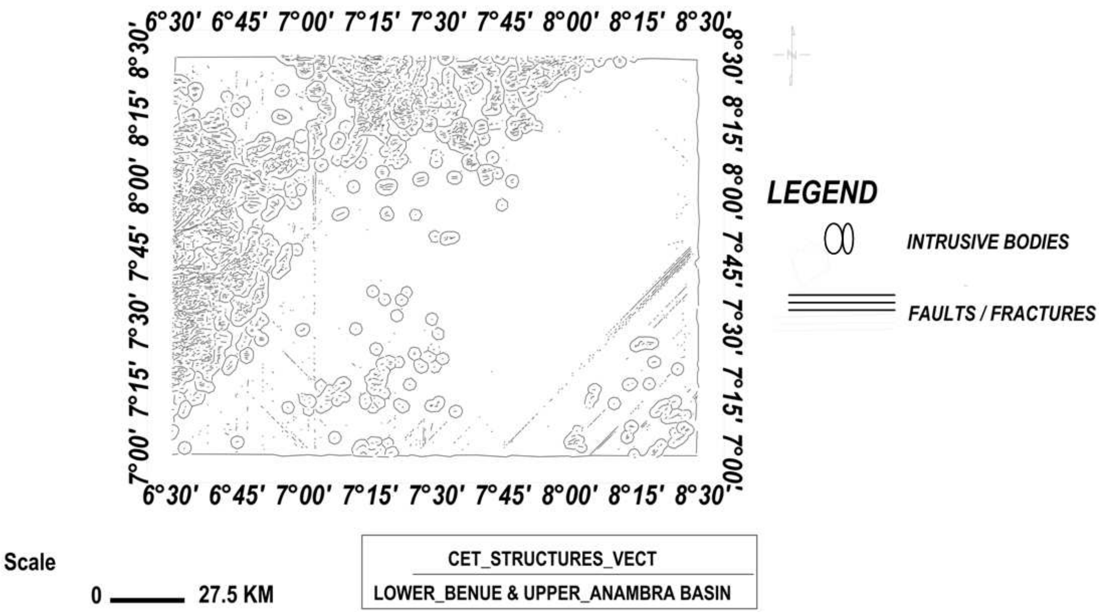

Fig 7: *Structural Map of the Study Area from CET Plug-in*

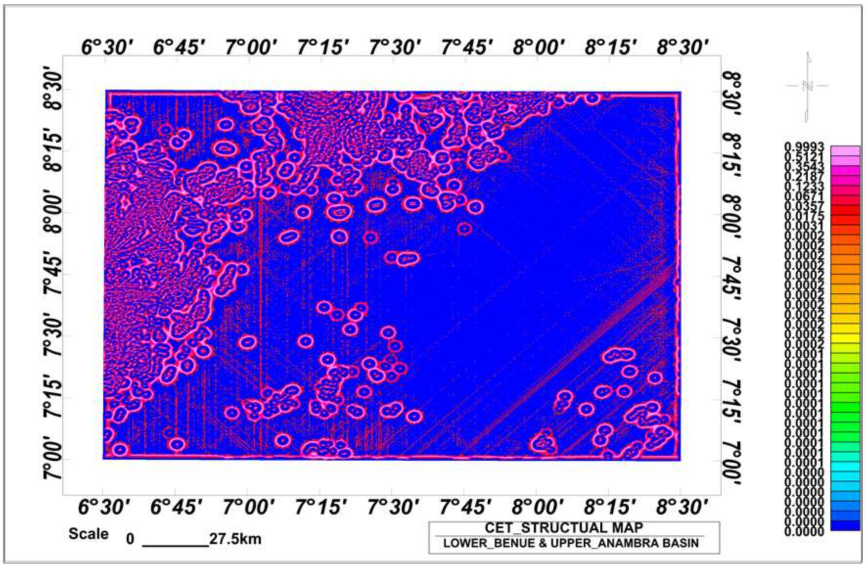

Fig 8: *Lineament Map of the Study Area from (CET) Grid Analysis*

5. Conclusions

From the vertical derivative map, Figure: 4, the nalytical Signal Map Figure: 6, and the Structural Map from CET Grid analysis Plug-in, Fig: 7, of the Study Area, the structural features in the area are as follow:-

The entire area can be divided into two lithology based on the signatures on the maps;

(A) The northern portion down to the western edge of the map is predominantly occupied by shallow base high frequency short wave anomalies which associated with basement signatures. Most of the structures identified at the northern edge of the map are trending NW-SE. this is in agreement with [15]. It is observed that from latitude 7.45^0 down to the 7.15^0 the structural trend changes to E-W trending this trend was also observed [16].

(B) The remaining portion of the map from the North-eastern edge of the map cutting the map into half down to the South-western edge. This right portion of the map is associated with low frequency long wavelength anomalies running E-W in direction. The northern portion of the map typically with basement structure is clearly separated from the southern portion whose features are predominantly of sedimentary basin. The contact between these two geological mapping is clearly identified from the CET structural mapping.

We note here that the middle Benue Trough is a sedimentary basin, where the sedimentary sequences have been outlined [17]. The basement sedimentary boundary is fairly defined from the Horizontal Derivative map Fig: 5 and the intrusive bodies on the Analytical Signal Map Fig: 6, based on the level of disruption of the field lines at the boundary. The Lower Benue Trough which is genetically related to the entire Benue Trough which itself is part of the west African Riff Subsystem [18].

The result of this research has identified three main structures that points at the mechanisms that is associated with the depression which allows accumulation os sediments that led to the formation of both the Anambra and Lower Benue Basins, which are:-

1. The major structural trend observed within the study area, which are NE – SW(at the upper part of the area) and E – W (at the lower part of the area) Figures: 3,4.5,and Fig:6, coupled with the direction of fault line identified in the study area on Fig: 4 and that observed from the CET grid analysis in Fig : 7 that strike NE – SW, indicates, a rifting and spreading of continental plates, a process that results in spreading tractions in the earth's crust and create some lineaments and faults along which long and narrow depressions bounded by steep slopes occur [18,19].
2. A major vertically fault line that structurally define the course of river Niger within the study area, and the extension of Chain's fault line that cuts the South East corner of the study area Fig: 7 coupled with the the presence of a basement uplift (Abakaliki uplift) adjacent to the study area cerate's an Isostatic adjustment of the graben-sag along week fault zones as blocks sink down in response to the traction, giving a depression which sediments can accumulate. [19].
3. Considering the existence of intrusive structures of Basaltic rocks within the lower portion of the study area oround Udegi and Angba , as reveal by Analytical Signal and CET grid analysis,Fig: 6 and Fig: 7 a region where the maximum thickness of sedimentation is observed, support the theory of intrusion of dense material such as basaltic intrusion into crustal rocks, this emplacement will act as a weight. During isostatic adjustment a depression is created on the surface directly above the dense material where sediments can accumulate [19].

References

[1] Colin Reeves. 2005 Aeromagnetic Surveys Principles, Practice and Interpretation, Section 2 pp 1- 22.

[2] Colin Reeves. 1985. The Kalahari Desert, central southern Africa – a case history of regional gravity and magnetic exploration. *In* Hinze, W.J. (ed), The utility of gravity and magnetic surveys, Society of Exploration Geophysicists, special volume, pp 144-156.

[3] Barbosa, V. C. F., Silva, J. B. C., and Medeiros, W. E. (1999) Stability analysis and improvement of structural index estimation in Euler deconvolution: *Geophysics,* 64, 48–60.

[4] Ojoh K. A. (1992) The Southern part of the Benue Trough (Nigeria) Cretaceous stratigraphy, basin analysis, paleo-oceanography and geodynamic evolution in the equatorial domain of the south Atlantic. NAPE Bull 7:131-152

[5] Petters S. W., Ekweozor C. M. (1982) Petroleum geology of the Benue Trough and South-Eastern Chad Basin, Nigeria. AAPG Bull 66:1141–1149

[6] Thompson, D. T. (1982) “EULDPH” A new technique for making computer-assisted depth estimates from magnetic data: *Geophysics*, 47, 31-37.

[7] Reid, A.B., Allsop, J. M., Granser, H., Millet, A. J., and Somerton, I. W. (1990) Magnetic interpretation in three dimensions using Euler deconvolution: *Geophysics,* 55, p. 80-91.

[8] Barbosa, V. C. F., Silva, J. B. C., and Medeiros, W. E. (1999) Stability analysis and improvement of structural index estimation in Euler deconvolution: *Geophysics,* 64, 48–60.

[9] Nabighian, M.N., 1974. Additional comment on the analytic signal of two dimensional magnetic bodies with polygonal cross-section. Geophysics, 39, 85-92.

[10] Nabighian, M.N., 1972. The analytic signal of two dimensional magnetic bodies with polygonal cross-section: its properties and use for automated anomaly interpretation. Geophysics, 37, 507-517.

[11] Peter Kovesi, P. (1997) “Symmetry and asymmetry From local phase”, AI’97, Tenth Australian. Joint Conference on Artificial Intelligence. 2 - 4 December 1997.

[12] Peter Kovesi, “Image features from phase congruency”, *Videre: Journal of Computer Vision Research*, Summer 1991, Volume 1, Number 3, The MIT Press.

[13] Akande, S, O and Erdtmann, B. D. (1998) Burial Metamorphism (Thermal Maturation) in Cretaceous sediments of the Southern Benue Trough and Anambra Basin, Nigeria: A.A.P.G. Bulletin v. 82,p.l191 – 1206

[14] Nabighian, M.N., 1974. Additional comment on the analytic signal of two dimensional magnetic bodies with polygonal cross-section. Geophysics, 39, 85-92.

[15] Avbovbo A. A., Ayoola E. O., Osahon G. A. (1986) Depositional and structural styles in the Chad Basin of northeastern Nigeria. AAPG Bull 70:1787–1798.

[16] Benkhelil, J. (1989) The origin and evolution of the Cretaceous Benue Trough, Nigeria. J Afr Earth Sci 8:251–282

[17] Nabighian, M.N., 1972. The analytic signal of two dimensional magnetic bodies with polygonal cross-section: its properties and use for automated anomaly interpretation. Geophysics, 37, 507-517.

[18] Reyment R Aand Dingle R V 1987 Palaeogeography of Africa during the cretaceous period palaeogoegr palaeoclimatol palaeocol 59, 93-116

[19] Beaumont C (1978) The evolution of sedimentary basin on a viscoellastic lithosphere theory and example *Geophys J ?Roy AstrSoc* 55,471-497